Assessing movement-specific resilience of a signalized road network under lane-level cascading failure

Physica A 654 (2024) 130154

Contents lists available at ScienceDirect

Physica A

journal homepage: www.elsevier.com/locate/physa

Assessing movement-specific resilience of a signalized road network under lane-level cascading failure

Guizhen Chen [a,b], Tom Van Woensel [b], Jinhua Xu [a], Yikai Luo [a], Yan Li [a,*]

[a] School of Transportation Engineering, Chang'an University, Xi'an, 710064, China
[b] Department of Industrial Engineering & Innovation Sciences, Eindhoven University of Technology, Eindhoven, P.O. Box 513, 5600 MB, Netherlands

ARTICLE INFO

Keywords:
Movement-specific resilience
Lane-level cascading failure model
Dual graph
Resilience assessment
Transportation network

ABSTRACT

Accurately assessing the resilience of the road network is crucial for responding to emergencies and enhancing public safety. Signal control plays a significant role in managing traffic flow. However, its impact is often overlooked in resilience assessments, where traffic flow and signal control are usually considered separately. A Movement-Specific Resilience (MSR) assessment model is proposed to integrate signal timing into resilience analysis. To accurately represent traffic flow paths under phase control, a dual graph is used to depict the topological network, allowing the assessment of relationships among all movements at an intersection. Based on this, a cascading failure model is developed to analyze the impact of signal control on traffic flow reassignment, reflecting how signal timing influences traffic flow propagation after failures. The method is validated using data collected from a sub-road network in Xi'an city. Results reveal the cumulative resilience of single lanes is not equivalent to the resilience of road segments. The MSR is higher when the network's failure degree is low and decreases as the failure level increases. Furthermore, road saturation is inversely related to MSR, while MSR is proportional to capacity. MSR remains unaffected by failures and oversaturation when capacity exceeds a certain threshold. These insights could be a theoretical foundation for bolstering resilience via signal control adjustments.

1. Introduction

A resilient transport network can have a greater ability to withstand disturbances, absorb external shocks, and recover itself [1]. Accurate resilience assessments are essential for informing transportation management strategies, enabling networks to recover quickly from disturbances and maintain safety during emergencies [2]. Traditional resilience assessment models typically evaluate road segment flows, assuming traffic can move freely between spatially interconnected road segments or lanes [3–5]. However, this approach overlooks a critical factor: the influence of signal control at intersections. Signal control significantly adjusts the temporal and spatial order of traffic passing through intersections, affecting the actual movement trajectories of vehicles [6–8].

Furthermore, due to the interconnected and interdependent nature of urban road networks, disturbances can cause cascading failures that propagate throughout the network [9]. The resilience of a transportation network can be measured by comparing its performance before and after a disturbance [10]. Cascading failure models analyze how congestion and failure spread following a disturbance to evaluate network performance [11], simulating the redistribution of extra traffic flow based on the weights of nodes or edges to analyze congestion and failure propagation. However, these models often fail to account for the influence of signal

* Corresponding author.
E-mail address: lyan@chd.edu.cn (Y. Li).

https://doi.org/10.1016/j.physa.2024.130154
Received 20 June 2024; Received in revised form 5 September 2024
Available online 9 October 2024

control on the paths and intensities of traffic propagation during disturbances. This oversight can lead to incorrect assessments of congestion points and failure propagation patterns, resulting in inaccurate resilience assessments.

In resilience analysis, transportation networks are often abstracted to topological networks. Topological networks, whether undirected or directed, weighted or unweighted, are constructed to analyze performance changes following a cascading failure, with nodes and edges depicting intersections and road segments, respectively [12,13]. The primary graph approach, commonly used in these models, can represent the green duration and phase sequence by adding node attributes. However, node attributes contain extensive information, which can complicate the topological structure when representing movement in large networks. A simplified but comprehensive approach is needed to characterize these dynamics effectively.

We need to consider three issues when assessing the resilience of transportation networks: (1) Current resilience assessment models primarily focus on the impact of road segments or lanes on traffic propagation, with limited attention given to traffic movements. (2) Existing cascading failure models applied in the resilience analysis fail to incorporate the influence of signal control at intersections on traffic flow congestion and failure propagation. (3) While assessing resilience, the efficacy of the primal graph method becomes complex when representing signal timing's role in regulating traffic flow in a topological network.

Therefore, this research proposes a Movement-Specific Resilience (MSR) assessment model incorporating signal control. This model focuses on traffic movements — defined as specific flow directions at intersections [14] — rather than just road segment flows. By analyzing these movements, we can more accurately assess network resilience, aiming to provide both theoretical advancements and practical guidance for system resilience. The main contributions of the study can be summarized as follows:

1. The development of an MSR assessment framework that assesses network resilience by focusing on the actual movement trajectories under signal control, providing a more accurate representation of traffic flows.
2. The cascading failure model is improved by analyzing lane cascading failures and the impact of signal timing on traffic propagation. This includes integrating signal timing parameters into reassignment rules and identifying the traffic propagation process for each lane after a failure.
3. The transportation topological network modeling technique advances by adopting a dual graph method to represent the signal-controlled network. This method adapts the topological network to reflect movement inherently, simplifying the characterization of complex transportation networks.

The remainder of the paper is organized as follows: Section 2 discusses a review of related literature. The methodology of the proposed MSR assessment model is described in Section 3. The dynamics of MSR with different parameters are presented in Section 4. Finally, Section 5 summarizes the research results of this paper and the outlook for future research.

2. Literature review

This section reviews and summarizes the literature on the transportation network resilience model. It consists of three parts: methods for building topological networks, cascading failure models for analyzing network performance after disturbances, and the definition and assessment methods for resilience.

2.1. Network modeling methods

Establishing topological networks is essential for accurately representing and analyzing the structure and dynamics of road network systems. Common road network modeling methods include primal-graph, dual-graph [15], and dynamic-graph approaches [16]. In the primal-graph approach, intersections are represented as nodes and road segments as edges, providing a simple and intuitive topological representation [17]. In contrast, the dual-graph method abstracts the network by representing intersections as edges and road segments as nodes [18]. The dynamic-graph method typically builds on the primal or dual-graph methods, with the graph's structure and weights changing over time [16]. The key difference between these three methods lies in how intersections and road segments are mapped. This difference influences their applicability in various types of road network analyses.

The primal-graph method used for constructing urban road topologies is straightforward. It directly reflects the physical layout of the road network, making it suitable for basic road network analysis. However, a single primal graph cannot accurately reflect the movement within the road network. The dual-graph method can analyze the space relationships between road segments with more detail [18]. The dual-graph method can characterize the traffic flow direction of a road segment by creating adjacency matrices between nodes. Creating a feature matrix for the edges can also assess the signal states.

2.2. Cascading failure model

Traffic network cascading failure occurs when a road segment or intersection malfunctions and triggers a redistribution of traffic flow to surrounding areas. This redistribution can lead to congestion and, in severe cases, may result in the loss of functionality across the entire traffic network zhang2023cascading. Several models have been developed to analyze such failures, including the load-capacity model [19], coupled map lattices model [20], percolation theory [21], sandpile model [22]. The load-capacity and coupled map lattice models are most commonly used due to their versatility.

Traditional road network cascading failure models typically focus on the impact of road segment or intersection failures on the entire road network. The load-capacity model simulates how traffic redistributes when a road segment or intersection fails. The critical steps of this model include four parts, which are (i) defining the initial load, (ii) defining the capacity, (iii) determining

attack strategy, and (iv) implementing a load reassignment strategy [23]. As research has progressed, studies have focused on the impact of directional traffic flow failures on the road network. In bidirectional road networks, the coupled map lattices model analyzes the failure of road segments and explores how interactions between traffic flows in different directions influence congestion propagation [24]. This approach provides a more accurate description of how failure spreads across different traffic flow directions. Further research refines the analysis to lane-level failures. Lane-level failure analysis enables a more granular understanding of how the failure of individual lanes impacts entire road segments and the road network [19].

These studies have gradually deepened the analysis of cascading failures and their impacts on road networks. However, current research analyzes these factors in isolation, not comprehensively examining how traffic flow disturbances propagate through road networks. Therefore, this paper proposes an integrated approach that combines signal control with lane-level failure analysis. This combination enables a more comprehensive assessment of the overall performance of the traffic network under stress.

2.3. Transportation resilience assessment method

Resilience was first introduced in ecological systems [25]. The concept of resilience has been extensively researched and defined within transportation systems. The initial definition encompassed ten dimensions [26]. Subsequently, resilience has been applied across various transportation domains, encompassing railxu2021resilient, road [27], maritime [28], and aviation systems [29]. In the context of road networks, network resilience refers to the network's ability to maintain, recover, and adapt system functions after disturbances [10,30]. Robustness, redundancy, resourcefulness, and rapidity [31,32] were proposed and widely used in road network resilience studies, which reflect the system's absorptive, recovery, and adaptive capacity.

Two main approaches are used to quantify resilience. The first approach, performance-based assessment, quantifies resilience by comparing network performance indicators before and after disturbances. For example, local network speed is a performance indicator to analyze resilience under various traffic conditions [33]. The second approach, attribute-based evaluation, defines network resilience attributes metrics and evaluates resilience based on these metrics [34,35]. Common resilience attributes include absorptive, restorative, and adaptive capacity, which performance indicators can measure. Both approaches can utilize performance indicators, categorized as topological or traffic-related, or a combination. Topological indicators include metrics such as network connectivity [36], accessibility [37], betweenness centrality [38]. Traffic-related indicators include delay [39], redundant paths [40], traffic demand satisfaction ratio [41] and so on. Regardless of the chosen approach, these indicators are the quantitative basis for assessing network resilience. The Table 1 summarizes the various evaluation objectives, methods, and corresponding indicators used in resilience assessment.

Road network resilience assessment typically focuses on the overall network's performance. These analyses examine the network's capacity to respond to natural disasters or significant traffic incidents, informing targeted improvement measures to enhance system-level resilience. While assessing the entire network is crucial, it often does not account for the specific impacts of critical road segments. Therefore, critical road segment resilience is proposed and studied in more detail [33] . However, in actual road design, multiple bidirectional lanes exist on a single road segment. The failure of a single lane cannot be equated with the failure of the entire road segment. To better understand this nuance, lane-level resilience is proposed [19] to explore the road network's ability to withstand single-lane failures. However, focusing on road segment or lane flow analysis overlooks the influence of signal control on traffic, which is critical to understanding overall traffic movement. Therefore, shifting the focus from segment-based or lane-based flow to studying movement across the network is essential. This shift allows for developing a Movement Specific Resilience (MSR) assessment framework. By incorporating signal control factors, this framework provides a more detailed and comprehensive assessment of network resilience. The MSR assessment approach advances our understanding of road network performance under disruptions and provides a theoretical foundation for enhancing resilience through signal control.

3. Methodology

This section outlines the framework for assessing MSR, including traffic topology network modeling, lane cascading failure modeling, and an MSR assessment model.

3.1. Framework for assessing the MSR

A model for assessing resilience that considers the effects of signal control in traffic regulation is proposed. The framework entails several vital steps as depicted in Fig. 1.

Initially, the topology of the signal-controlled transportation network is established using a dual graph, where intersections are mapped as edges and lanes as nodes. Then, the process of lane cascading failures is analyzed, which consists of three main parts: defining the initial network's capacity and flow using a load-capacity model, discussing node attack and edge attack strategies, and integrating signal control parameters into the reassignment model to analyze the process of traffic flow spreading from failed lanes to adjacent lanes. Finally, based on the network performance before and after failure, the MSR is evaluated using the metrics of Lane Absorption Capacity (LAC), Lane Recovery Capacity (LRC), and Lane Adaptation Capacity (LDC). Table 2 defines the parameters employed within this resilience assessment framework.

Table 1
Literature on transportation network resilience assessment.

Performance-based measurement			Attributes-based measurement			
Failure scenarios	Research subjects	Performance indicators	Failure scenarios	Research subjects	Attribute metrics	Performance indicators
Road segment failure	Transportation network	Time and cost required to restore component [10]	Road segment failure	Transportation network	Adaptive resilience	Performance [42]
Road segment failure	Transportation network	Link reliability, network stability [43]	Road segment failure	Transportation network	Throughput resilience, O-D connectivity resilience, average reciprocal distance resilience	Average degree, diameter, cyclicity [37]
Road segment failure	Road network	Speed [33]	Road segment failure	Road network	Adaptive capacity, relative size of the giant component	Betweenness centrality, node strength, adaptive capacity [44]
Road segment failure	Road network	Delay [39]	Road segment failure	Road network	Absorption capacity, recovery capacity	Independent paths, redundancy of the network [45]
Road segment failure	Road network	Equivalent resistance, survival Function [40]	Road segment failure (bidirectional)	Transportation network	Connectivity reliability, vulnerability	Flow, link importance [46]
Road segment failure	Road network	Travel time, shorten path [27]	Lane failure	Road network	Resilience performance index, the robustness index, the recovery index	Traffic flow [19]
Road segment failure	Public transit system (bus)	Travel time, volumes [47]	Node failure	Public transit system (Rail transit network and bus)	Resistance, recoverability, adaptability	Structural resistance, structural recoverability, functional resistance, functional recoverability, passenger adaptability, management adaptability [48]
Node failure	Air transportation network	Flight connectivity, delay connectivity [49]	Node failure	Air transportation network	Vulnerability, emergency capability	The class and scale of airports, operation intensity, the scale of the flight area, passenger arrival rate, maximum number of takeoffs and landings, and the scale of security infrastructure [29]
Node failure	Maritime transportation network	Network density, network centrality, network connectivity, network size [50]	Node failure	Maritime transportation network	Robustness, redundancy, visibility, flexibility, agility recovery	Network structure [51]

(*continued on next page*)

3.2. Transportation network topology modeling

The topology structure of the transportation network, based on a dual graph, can be represented as a directed, weighted network, denoted as $G = \langle N, E, A, T \rangle$. In this representation, $N = \{N_i\}$ is the set of nodes in the topology network, where each node N_i

Table 1 (*continued*).

Node failure	Maritime transportation network	Node centrality, edge betweenness centrality, transmission Efficiency [38]	Node failure	Maritime transportation network	Absorption capacity, adaptive capacity, restorative ability	Additional capital equipment, alternate routing, timely evacuation, relocation, conservation, facility restoration, manpower (service) restoration, technology restoration [28]
Node failure	Rail transit network	Network efficiency, bi-directional passenger flow [36]	Node failure	Rail transit network	Absorption ability, resistance ability, recovery ability	Global efficiency, passenger flow [52]
Node failure	Rail transit network	Global Efficiency, topological Integrity, importance exposure (demand, travel time)[53]	Node failure	Rail transit network	Preparedness, robustness, recovery, adaptation	Node degree, node flow, flow-weighted betweenness centrality [54]

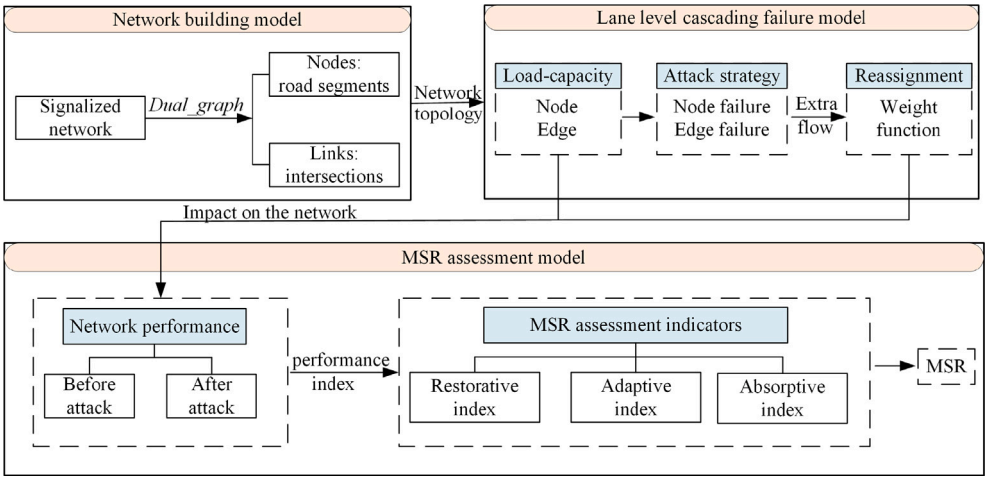

Fig. 1. MSR assessment framework.

corresponds to a specific road segment. Each road segment N_i can be further decomposed into lanes, represented as N_{i_k}, indicating the individual lanes within segment N_i. The set of directed edges $E = \{E_{i\to j}\}$ represents the edge set of the network topology. These edges indicate the movement from the upstream direction(road segment) i to the downstream direction(road segment) j, controlled by the intersection phase. The adjacency matrix $A = \{a_{i\to j}\}$ indicates the connections between directions, with $a_{i\to j} = 1$ signifying an allowed movement from direction i to direction j, and $a_{i\to j} = 0$ indicating no allowed movement. Fig. 2 represents the difference between the primal and dual graph approaches in representing the same road network. Fig. 2(a) shows the original road network, where the arrows indicate the permitted movement directions under signal control. Fig. 2(b) represents the topological road network created using the primal graph method, which describes the spatial relationships between road segments and intersections. Fig. 2(c) illustrates the topology constructed using the dual graph method. In this representation, the short dashed lines represent movements through intersections when traveling straight. The long dashed lines indicate movements associated with right turns, and the solid lines depict movements involving left turns. This dual representation effectively captures the spatial relationships between road segments and intersections under phase control.

The flow matrix from segment i to segment j is denoted as W (see Eq. (1)).

$$W = \begin{bmatrix} w_{1\to1} & w_{1\to2} & \cdots & w_{1\to N} \\ w_{2\to1} & w_{2\to2} & \cdots & w_{2\to N} \\ \vdots & \vdots & \ddots & \vdots \\ w_{N\to1} & w_{N\to2} & \cdots & w_{N\to N} \end{bmatrix} \tag{1}$$

where $w_{i\to j}$ represents the movement per time step.

Table 2
Variables and parameters used.

Notation	Definition
R_{abs}	Performance of lane degradation after attack
R_{abt}	Lane performance degradation time after attack
R_{res}	Performance of lane restoration after attack
R_{ret}	Lane performance restoration time after attack
R_{ada}	Performance of lane adaption after attack
$F(t)$	Lane Performance at t time
s_t	Lane saturation when the lane is not under attack at t time
$s_t^{'}$	Lane saturation when the lane is under attack at t time
μ	The capacity tolerance parameter, $0 < \mu < 1$
$\Delta x_{i\to j}$	Redundant flows in movement $E_{i\to j}$ resulting from the failure of direction i
$Q_{i\to j}$	The initial load of the movement $E_{i\to j}$
$S_{i\to j}$	The saturation flow rate of the movement from direction i to j
$\lambda_{i\to j}$	The green ratio for a specific movement $E_{i\to j}$ within a signal cycle
$g_{i\to j}$	The effective green time for the movement $E_{i\to j}$
$y_{i\to j}$	The cycle length
M^i	The set of upstream neighbors associated with the failed direction i
$C_{i\to j}$	The capacity for a single traffic movement $E_{i\to j}$, defined by the maximum number of vehicles that can pass during the green phase
$P_{i\to m}$	The expected weight assigned to the redundant traffic flow from failed direction i to upstream m
$\Delta x_{i\to m}$	Additional traffic flow assigned from failed segment i to m
t_e	Disturbance onset time
t_d	Performance nadir time
t_r	Functional recovery time
η_1, η_2, η_3	Weight coefficients

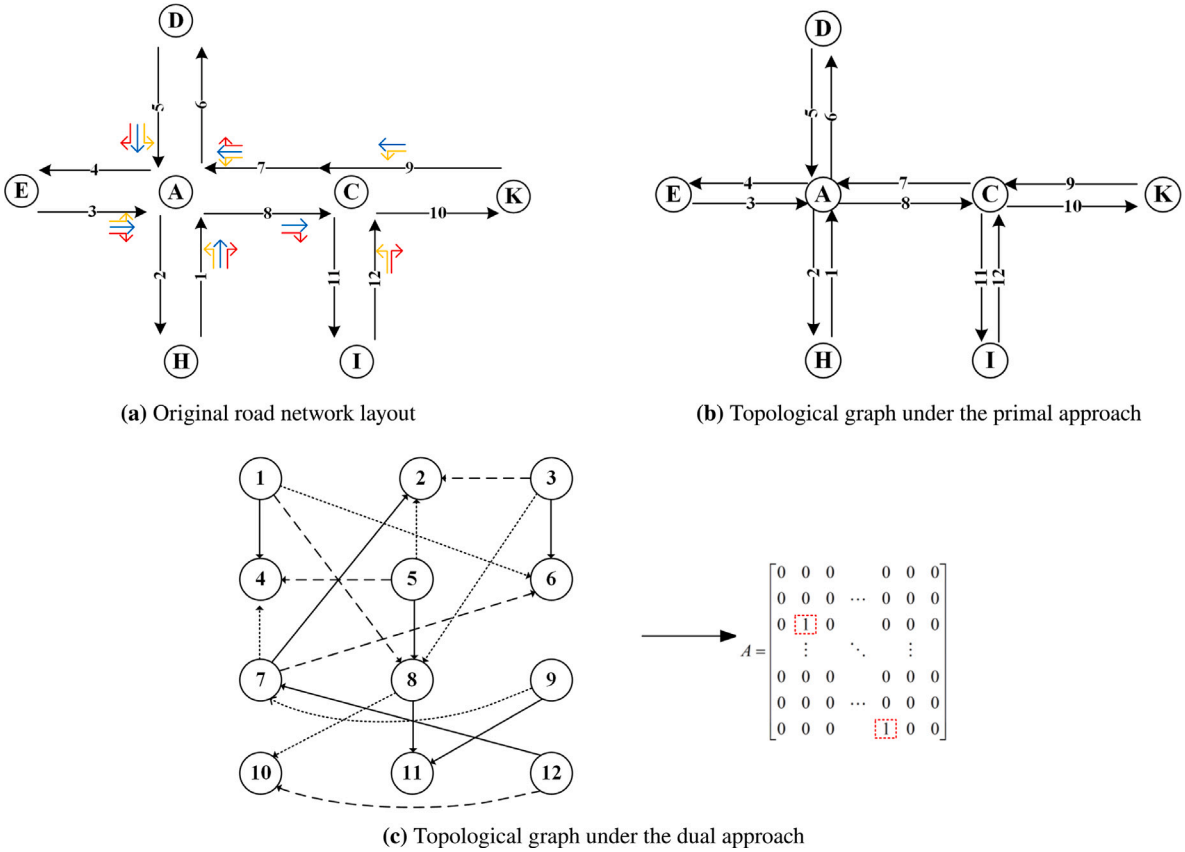

(a) Original road network layout

(b) Topological graph under the primal approach

(c) Topological graph under the dual approach

Fig. 2. Illustration of the initial road network and the topological representations under different graph approaches.

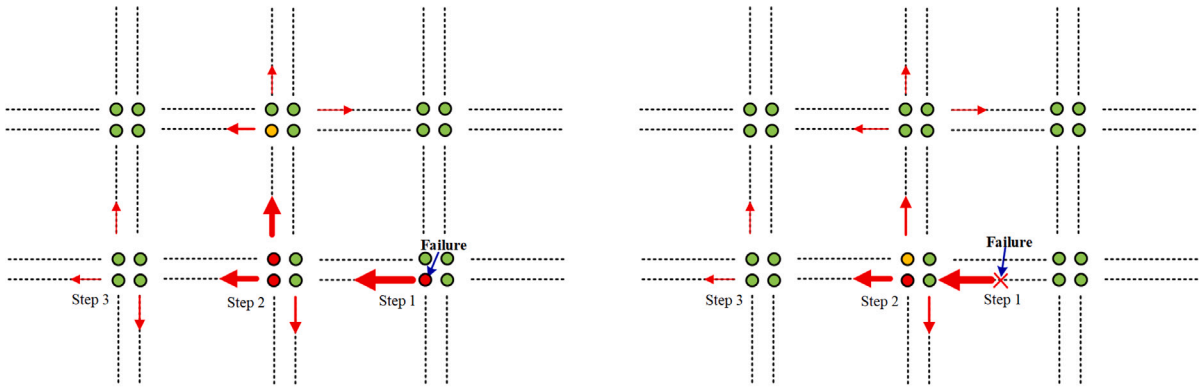

(a) Congestion propagation process under intersection attack **(b)** Congestion propagation process under lane attack

Fig. 3. Cascading failure process under attack.

3.3. Lane level cascading failure model

3.3.1. The load-capacity model

The load-capacity model analyzes the cascading failure in transportation networks [19,23] . In our study, the initial edge load $Q_{i\to j}$(intersection load) is defined as the total flow transitioning from segment N_i to segment N_j per time step, referred to as the particular traffic movements. The edge's capacity $C_{i\to j}$ (intersection capacity) is influenced by two main factors: the maximum rate at which vehicles can pass through the intersection(also known as the saturation flow rate $S_{i\to j}$) and the green time ratio $\lambda_{i\to j}$ in signal timing during which vehicles are allowed to enter [55,56] . It is the maximum number of vehicles it can handle for a single traffic movement per time step. Following the Highway Capacity Manual (HCM) guidelines [14], the capacity $C_{i\to j}$ can be expressed as in Eq. (2).

$$C_{i\to j} = (1+\mu)S_{i\to j}\lambda_{i\to j} \tag{2}$$

Here, $S_{i\to j}$ is the saturation flow rate, μ is a capacity tolerance parameter, and $\lambda_{i\to j}$ is the green ratio, defined as:

$$\lambda_{i\to j} = \frac{g_{i\to j}}{y_{i\to j}} \tag{3}$$

where $g_{i\to j}$ is the effective green time and $y_{i\to j}$ is the cycle length.

3.3.2. Attack strategy

Fig. 3 illustrates the cascading failures triggered by intersection and lane attacks. The red arrows indicate the direction in which congestion propagates following a disturbance.

A. Intersection attack Failures in transportation networks can typically be categorized into two types: congestive failures and complete failures. When an intersection fails, it initiates congestion in the connected lanes. This congestion then progressively extends to adjacent intersections, causing a chain effect over time. It is important to note that congestive failures at neighboring intersections do not necessarily lead to complete failure, as the system attempts to handle the additional traffic load. This cycle persists until the intersections and road segments can effectively accommodate the traffic demand.

B. Lane attack Transportation road networks are complex systems consisting of multi-lane roads. In the dual graph representation, failures within road segments are naturally represented by the failure of specific nodes. Therefore, for simplicity and consistency, our study assumes that these road segments are typically separated by medians, which can prevent disturbances in one direction from directly affecting the opposite direction. Consequently, failures within these road segments can be categorized into two main categories: two-way and one-way lane failures, further divided into all-lane and single-lane failures.

In the case of a two-way lane failure, congestion spreads to upstream intersections and impacts traffic flow in both directions. On the other hand, if a one-way lane fails, congestion will also propagate towards the upstream intersection since the traffic flow in the failed lane comes from various upstream movements, which are influenced by signal timing. Traffic can only move when the signal phase permits. Thus, the spread of congestion is similarly impacted by it. Even a single-lane failure can impact the adjacent lanes' operational efficiency and contribute to congestion spreading toward the upstream intersection.

The cascading failure continues until the affected intersection and all lanes can handle traffic demands effectively.

Table 3
Comparison between movement-specific resilience model and resilience triangle model.

Aspect	Resilience triangle model	MSR model
Analysis level	Macro-level system performance	Movement-specific analysis
Signal control consideration	Not typically considered	Explicitly integrated
Cascading failure representation	Assumes uniform impact across road segments	Congestion spread with integrated signal timing
Topological network representation	Primal graph method	Dual graph method
Urban adaptability	Limited	Specifically designed for urban complexities

3.3.3. Traffic assignment strategy

The redundant traffic flow $\Delta x_{i\to j}$ from the failed movement ($E_{i\to j}$) will transfer to the upstream neighbor directions in proportion to their remaining capacity [19,23]. Congestive failure occurs when an intersection becomes over-saturated. A factor $\gamma_{i\to j}$ is usually set to balance intersection efficiency and green time utilization. Therefore, to ensure the effective utilization of the intersection or lanes, its load must remain within this threshold, as represented by $\gamma_{i\to j}C_{i\to j}$. The redundant flow can be expressed as Eq. (4):

$$\Delta x_{i\to j} = Q_{i\to j} - \gamma_{i\to j}C_{i\to j} \tag{4}$$

Here, i and j represent movement directions, where j is the downstream direction of i.

The propagation of congestion following a failure is influenced by signal control due to the timing and phase sequence at intersections. Signal control directly affects the flow rates and the accumulation of vehicles from the upstream intersections. When congestion occurs, the direction and proportion of its spread to upstream directions are heavily influenced by signal timing. The impact factor $\lambda_{m\to i}$, representing the green movement ratio from upstream m to downstream i, should be incorporated into the original reassignment model. This integration is necessary to account for the influence of signal timing on congestion propagation. Therefore, the proportion of transferred redundant traffic from failed $E_{i\to j}$ to upstream can be represented as Eq. (5):

$$P_{i\to m} = \frac{(\gamma C_{m\to i} - Q_{m\to i})}{\sum_{m\in M^i}(\gamma C_{m\to i} - Q_{m\to i})}\frac{\lambda_{m\to i}}{\sum_{m\in M^i}\lambda_{m\to i}} \tag{5}$$

m represents the upstream direction of i, and M^i denotes the upstream neighbors associated with the failed direction i. Therefore, the extra traffic reassigned is calculated as Eq. (6):

$$\Delta x_{i\to m} = P_{i\to m} * \Delta x_{i\to j} \tag{6}$$

After the reassignment process, the traffic flow of intersection $E_{m\to i}$ is updated to $Q'_{m\to i} = Q_{m\to i} + \Delta x_{i\to m}$. At this time, if $\frac{Q'_{m\to i}}{Q_{m\to i}} \le \gamma_{m\to i}$, the intersection is considered operational. However, the intersection is considered failed if this ratio exceeds $\gamma_{m\to i}$. In such a case, the excess flow will spread to neighboring intersections and segments, and the flow at those intersections and segments will be reassigned iteratively again until the failure is resolved.

3.4. Movement-specific resilience assessment model

Movement-specific resilience (MSR) refers to the ability of a road network to absorb disturbances, recover to its original state, and adapt to new conditions when facing disruptions, focusing on analyzing traffic movements rather than segment flows. While sharing similarities with the widely used resilience triangle model, the MSR model offers several key advantages. Table 3 presents a detailed comparison.

The MSR model effectively captures performance changes based on lane failures, enabling targeted interventions to improve network resilience in complex urban settings. The performance change based on the lane failure is shown in Fig. 4.

Saturation can be used as a performance indicator to represent the operational status of the lane and intersection. High saturation levels generally indicate that the transportation system is operating inefficiently. As a result, we have determined that the most resilient systems experience the smallest reduction in performance indicators after a disturbance. The performance indicator, denoted as $F(t)$, can be calculated using Eq. (7) to assess the network performance at any given time t.

$$F_t = s_t / s'_t, \tag{7}$$

where s_t and s'_t indicate the function before and after failure at time t.

Lane Absorptive Capacity (LAC) refers to the ability of a lane to withstand the negative impacts of unforeseen incidents. This can be expressed in terms of the lane's lost performance R_{abs} and performance degradation duration R_{abt}. These factors are inversely proportional to the lane's absorption capacity.

$$R_{abs} = \int_{t_e}^{t} [F(t) - F(t+1)]\mathrm{d}t \tag{8}$$

where $t_e \le t \le t_d - 1$, t_e represents the time point at which the network's performance begins to degrade due to an attack, and t_d is the time point at which the network's performance reaches its lowest level.

$$R_{abt} = t_d - t_e \tag{9}$$

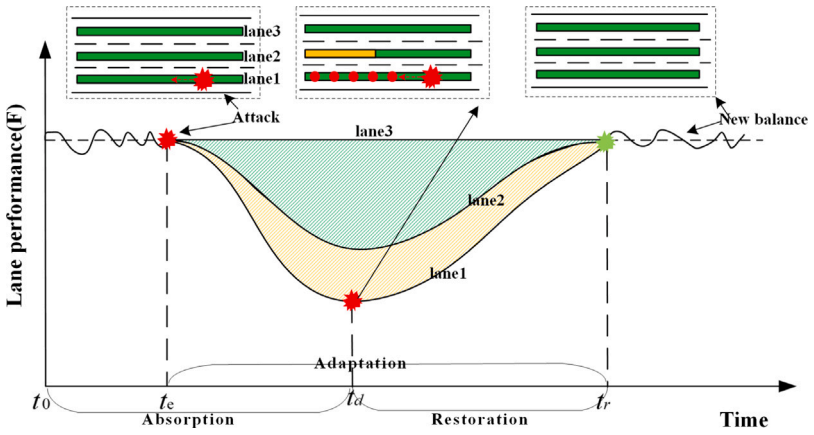

Fig. 4. Schematic representation of MSR.

Lane Restorative Capacity (LRC) measures the ability of a lane to resume its evacuation functions after a disturbance. Two main factors determine this capacity: the degree of recovery R_{res} and the time to recover R_{ret}. A lane's ability to restore its functions effectively is directly proportional to the speed at which it recovers.

$$R_{res} = \int_{t_d}^{t} [F(t+1) - F(t)]\mathrm{d}t \tag{10}$$

where $t_d \le t \le t_r - 1$, t_r represents the time point at which the network's performance begins to normal.

$$R_{ret} = t_r - t_d \tag{11}$$

Lane Adaptive Capacity (LDC) denotes a lane's capability to adjust to the new situation in the event of a disturbance. The ability of a lane to restore lost functionality (see the Eq. (12)) is used to measure a lane's adaptability R_{ada}.

$$R_{ada} = \frac{\int_{t_d}^{t_r} [F(t) - F(t_d)]\mathrm{d}t}{\int_{t_e}^{t_d} [F(t_e) - F(t)]\mathrm{d}t} \tag{12}$$

The three attribute metrics described above dynamically analyze the evolution of system performance changes. The Eq. (13) is utilized to evaluate MSR qualitatively.

$$MSR = \eta_1(1 - R_{abs}) + \eta_2 \frac{R_{res}}{t_r - t_d} + \eta_3 R_{ada} \tag{13}$$

where η_1, η_2, and η_3 denote the three indicators' weighting coefficient, which can be adjusted according to the management objectives.

In summary, Table 4 shows the procedures of calculating the MSR:

4. Case study

In this section, we validate the efficacy of the MSR assessment and conduct a sensitivity analysis. We designed eight failure scenarios to analyze the statistical characteristics of resilience and verify the model's effectiveness. Additionally, in the sensitivity analysis, we primarily investigate the impact of failure degree, road saturation, and intersection capacity on MSR.

4.1. Design of experiments

The road network in the southern part of Xi'an City, Shaanxi Province, China(see Fig. 5) is selected for the study. This area comprises 91 lanes across 21 intersections. The diversity of lane types in this network, such as bidirectional, unidirectional, tidal, and right-in/right-out lanes, provides a comprehensive basis for examining the process of lane disturbance.

Intersection signal timing and lane flows are investigated and used as information to establish the adjacency matrix, flow matrix, and weight matrix.

Various failure scenarios(see Table 5) are devised to evaluate the MSR. These scenarios compare the impacts of various failure types on MSR, such as lane failures versus section failures and unidirectional failures at intersections versus complete intersection failures. The failure scenarios are mainly assigned two categories: intersection failure and road segment failure. Intersection failure consists of intersection complete failure and intersection failure in a certain direction, while segment failure is categorized into entire road segment failure and single-lane failure. The results presented are based on the averages of 500 simulations.

Table 4
The process of calculating the MSR.

Input:
The adjacent matrix A
The traffic flow matrix W
Basic data of the urban road: service level, road distance, load and capacity
Capacity parameter: μ
Control threshold value: $\gamma_{i\to j}$
Signal control impact factor: $\lambda_{i\to j}$
Output:
The result of lane resilience: R_{abi}, R_{abs}, R_{res}, R_{ret}, R_{ada}, MSR
Initial settings:
Initialize the iteration number $t = 0$;
Step 1: Attack model: Intersection failure, Lane failure
Get the attack nodes or edges
Step 2: Cascading failure
Traffic reassignment: for the failure intersections or lanes, calculate the weight of reassignment of the neighborhoods intersections by Eqs. (4)–(5)
Then calculate the intersection flow after the distribution
Step 3: Recover
All failure intersections, process recover if saturation > threshold, then if the intersections fail, back to Step 2.
Until saturation < threshold
Step 4: For μ in (0.1, 1), calculate resilience by Eqs. (7)–(13)
End

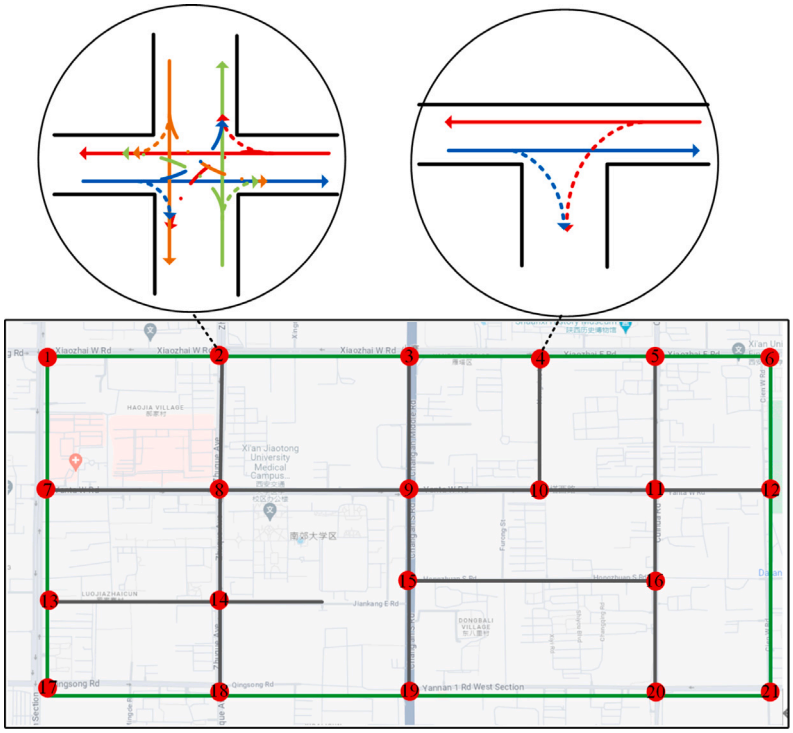

Fig. 5. Layout of studied transportation networks.

4.2. General characterization of MSR

The statistical characteristics of MSR, obtained by simulating the failure scenarios provided in Table 5, are shown in Fig. 6. The figure shows that system performance initially decreases after an attack on the road network but gradually returns to normal. This is because congestion spreads faster than the system's recovery mechanisms can handle. As congestion peaks, system performance drops. However, as the congestion spreads wider but with less intensity, the system stabilizes and eventually returns to normal.

The system performance analysis under eight different failure scenarios reveals a descending order of MSR: S4, S2, S3, S8, S1, S6, S7, S5, as displayed in Fig. 6(a). This ranking indicates that as the degree of failure increases, the system performance declines, and congestion lasts longer. Additionally, the recovery time extends. The duration of system performance degradation is longer than the recovery time, except for scenario S5. This phenomenon could be attributed to the pronounced degradation of system performance

Table 5
Selected different failure scenarios.

Scenario	All phase failure at the intersection	One phase failure at the intersection	Complete failure at the road section	Lane failure
Scenario1(S1)	1	0	0	0
Scenario2(S2)	0	1	0	0
Scenario3(S3)	0	0	1	0
Scenario4(S4)	0	0	0	1
Scenario5(S5)	1	0	1	0
Scenario6(S6)	0	1	1	0
Scenario7(S7)	1	0	0	1
Scenario8(S8)	0	1	0	1

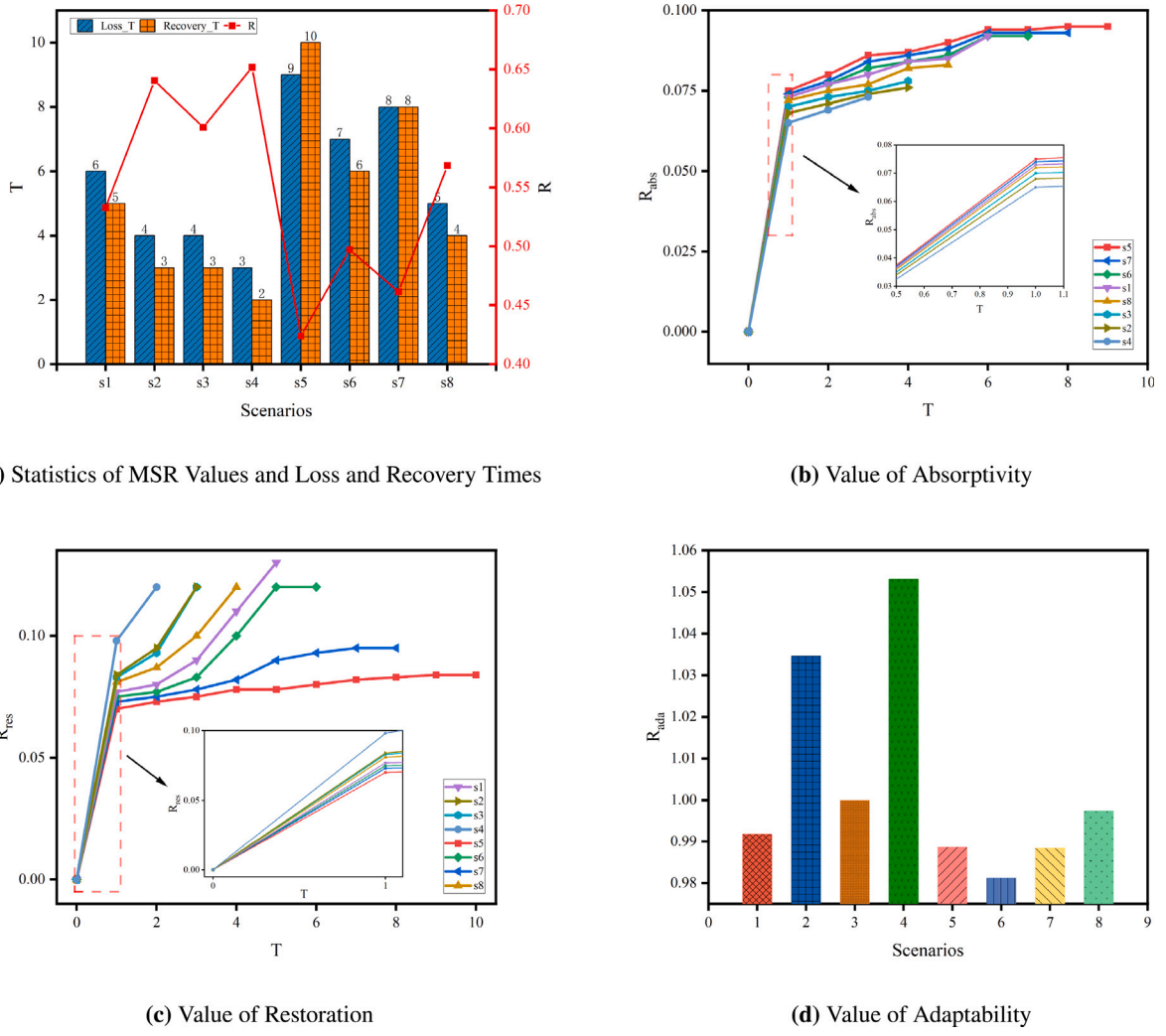

(a) Statistics of MSR Values and Loss and Recovery Times

(b) Value of Absorptivity

(c) Value of Restoration

(d) Value of Adaptability

Fig. 6. Resilience results analyzed under different failure scenarios.

in S5, which requires a longer recovery period. Scenario 4 exhibits a higher MSR than Scenario 2, while Scenario 3 exceeds Scenario 1 in MSR. These findings show that intersection failures have a greater impact on traffic efficiency than lane failures.

Fig. 6(b) illustrates the pattern of MSR degradation under the above eight failure scenarios, which helps us understand how congestion spreads within the network. Overall, the more failures there are, the worse the system performs. The spread of congestion is not linear. Initially, congestion spreads gradually because network redundancy slows down its spread. As congestion persists and spreads to adjacent lanes and intersections, its speed accelerates, leading to a faster decline in the overall performance of the road network until it reaches its worst state.

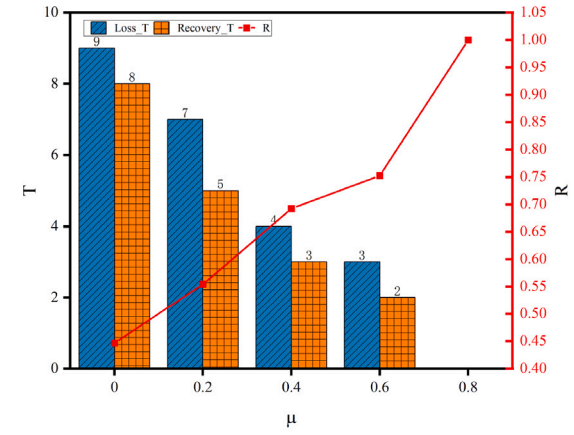

(a) Statistics of MSR Values and Loss and Recovery Times

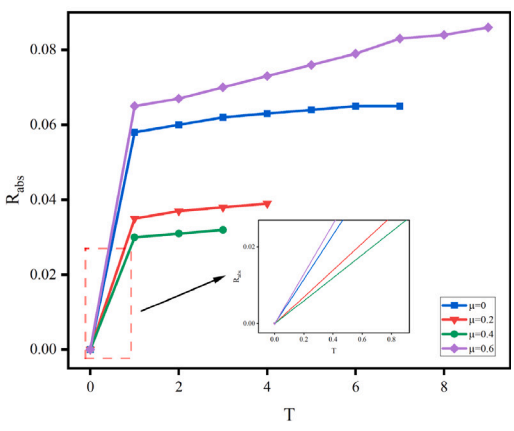

(b) Value of Absorptivity

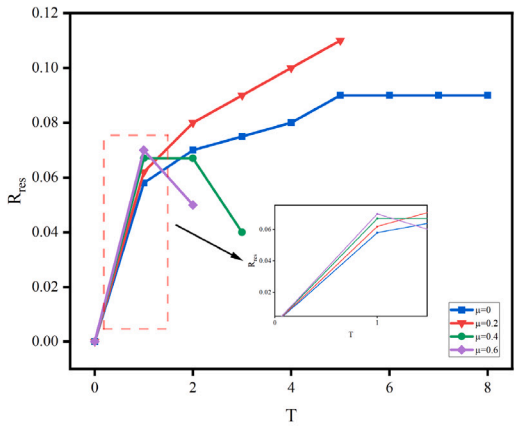

(c) Value of Restoration

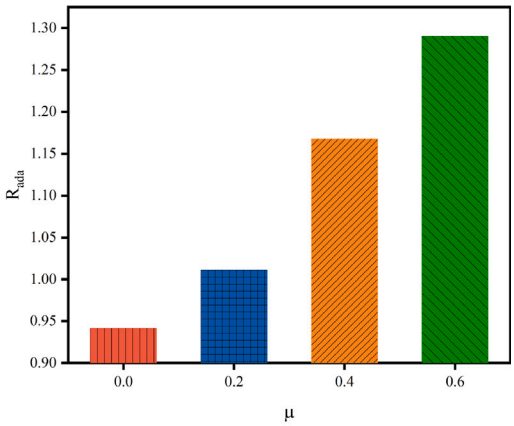

(d) Value of Adaptability

Fig. 7. Influence of capacity on MSR.

The recovery process following the system's lowest performance point is depicted in Fig. 6(c). An inverse relationship exists between the degree of failure and the system's restoration speed. The system's performance recovery rate increases with time. Initially, the congestion is at its worst, slowing the evacuation process. As the system performance improves, the speed of vehicle departure gradually increases, enhancing the efficiency of the recovery process.

The adaptability of the network is crucial in determining the system's performance after an attack on the network, which is illustrated in Fig. 6(d). This adaptability can either improve or worsen the overall system performance.

4.3. Influence of intersection capacity on MSR

Given the load-capacity model, the intersection capacity is pivotal in determining the MSR of a transportation network. The split and cycle length emerge as decisive parameters among the factors influencing intersection capacity. To simplify the analysis of how changes in intersection capacity affect MSR, we analyze the parameter μ to represent the intersection's capacity in a normalized form, where μ can be incremented by 0.1, and $\mu \in (0, 1)$.

Fig. 7 illustrates the relationship between the parameter μ and MSR in the event of lane failure. We discussed the changes in adaptive, absorptive, and restorative capacity under different values of μ.

Fig. 7(a) examines the dynamics of MSR for different values of μ. As μ increases, the time taken for failure and recovery decreases, and the MSR increases. This phenomenon occurs because a higher road capacity increases the redundant flow, which improves the system's ability to handle unexpected situations. It is essential to note that the system resilience reaches its maximum value of 1 when μ exceeds 0.8. This suggests disturbances have negligible effects on the system when the capacity is sufficiently large. As a result, we will not analyze the MSR performance metrics for values of μ greater than 0.8.

Fig. 7(b) shows that as μ increases, the redundant capacity at the intersection also increases. Consequently, there is a slower decrease in congestion propagation. A comparative analysis of R_{abs} across various μ values indicates the degradation in system performance is significantly reduced for $0.2 < \mu < 0.4$. This finding suggests that increasing capacity within this range may be most effective. This suggests that strategically increasing capacity can achieve the desired regulatory objective.

Figs. 7(c) show that the recovery rate increases as the parameter μ increases. However, the recovery rate decreases during the recovery process when $\mu = 0.4$ and $\mu = 0.6$. This phenomenon may occur because the system is approaching a fresh equilibrium, which results in a reduced recovery rate.

From Fig. 7(d), it is noted that as the value of μ increases, the network's performance of the new steady state achieved post-recovery also enhances. This improvement is attributed to the increased system redundancy capacity with the increase in the value of μ.

Comprehensive analysis indicates that intersection capacity (μ) significantly impacts the MSR of road networks. Increasing capacity enhances the system's adaptability, absorption, and recoverability while reducing recovery time. These findings provide theoretical support for developing transportation management strategies, demonstrating that optimizing intersection capacity settings can significantly improve network resilience in the face of disturbances.

4.4. Influence of saturation degree on MSR

The traffic flow varies depending on the time of day, with higher saturation during peak hours and lower saturation during off-peak hours. Lane failures are simulated during evening peak and off-peak hours to assess the dynamic MSR changes in transportation networks, with a specified parameter value of $\mu = 1.2$.

The analysis of Fig. 8(a) shows that the deterioration in evening peak performance surpasses that of the off-peak. This difference can be attributed to the heightened road traffic flow during the evening peak hours. During this peak period, the disparity between road and minimum performance is minimal, leading to a reduction in redundant traffic flow. As a result, even minor disturbances can cause system failure due to its limited performance tolerance. This phenomenon explains the inner degradation mechanism at peak and off-peak hours, as shown in Fig. 8(b).

The efficiency of system restoration and its adaptability across various saturation levels are compared in Figs. 8(c) and 8(d). The analysis reveals that the system recovery efficiency and adaptive capacity are higher during off-peak hours. The lower system load during off-peak hours means a large amount of redundant capacity is available for failure recovery and response. Moreover, the propagation of faults is relatively slower during off-peak hours, which leads to a faster system recovery process.

4.5. Sensitivity analysis

Many factors intricately influence the road network's performance, including the road system's operational state, the degree of failures, and the capacity of intersections. Collectively, these factors significantly influence the determination of MSR within the network.

The impact of varying failure degrees and capacities on MSR is depicted in Fig. 9. The figure elucidates that the capacity decreases as the failure degree increases, resulting in a proportional decrease in MSR. When the system experiences a failure degree above 0.5 and $0.1 \leq \mu \leq 0.7$, its performance declines rapidly. This observation suggests that even with a marginal increase in capacity, a significant degree of failure severely limits the enhancement of MSR. Therefore, the intervention of traffic authorities becomes crucial to facilitate and expedite the recovery of the road network.

The dynamic changes in MSR across different saturation and failure degree levels are illustrated in Fig. 10. Consistent with the preceding single-factor analysis findings, the road network demonstrates greater resilience at lower saturation degrees, effectively mitigating the impact of significant failures. In contrast, when the saturation degree surpasses 0.7, the system's resilience diminishes significantly. This highlights the need to monitor high-saturation lanes and road segments. Appropriate strategies can be adopted to prevent minor disturbances from escalating into widespread cascading failures.

Fig. 11 depicts the influence of both saturation and the capacity factor μ on MSR. The system recovery efficiency transitions from significant to marginal as saturation exceeds 0.7, with the capacity factor μ ranging between 0.1 and 0.7. This implies that increasing intersection capacity is an effective way to reduce initial congestion caused by unforeseen disturbances. However, once road saturation reaches a certain threshold, the impact of growing intersection capacity on congestion regulation becomes notably constrained. Alternative traffic management strategies have become more viable at this point. Different regulation measures should be used to optimize network resilience under different road operating conditions.

5. Conclusions

Movement-specific resilience assessment is crucial and necessary, as it integrates signal control features into the evaluation of network resilience. The concept of MSR is defined with assessment metrics including LAC, LRC, and LAC. The research enhances the cascading failure model by analyzing the lane failure and investigating the impact of signal timing on the failure process. A dual graph is utilized to construct a road topology network that inherently characterizes phase designs in signal control. This approach enhances the model's accuracy in reflecting a realistic transportation network. Furthermore, the study investigates the characteristics of the MSR assessment metrics under various failure scenarios. It analyzes the properties of MSR influenced by three key metrics: degree of failure, saturation, and capacity.

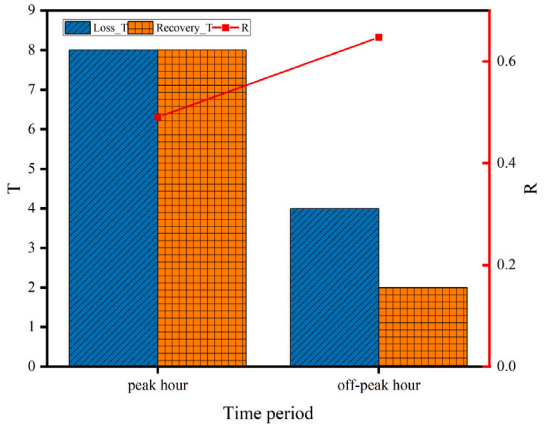

(a) Statistics of MSR Values and Loss and Recovery Times

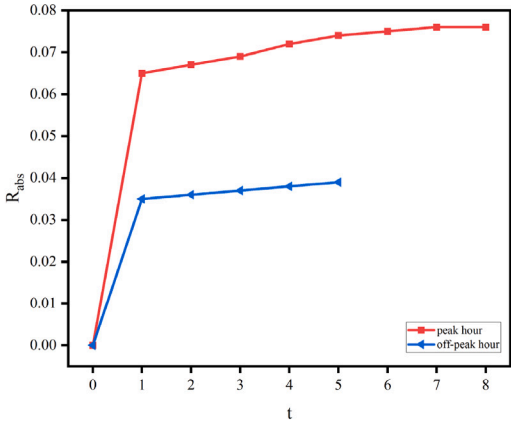

(b) Value of Absorptivity

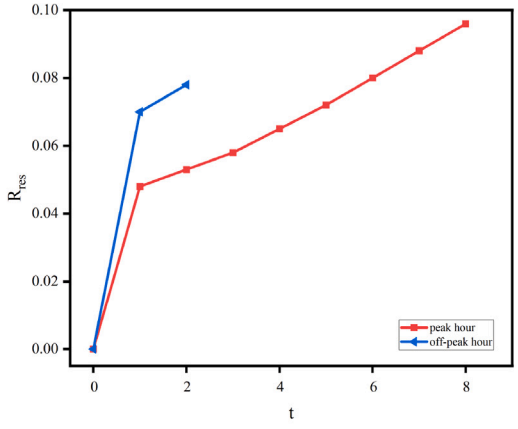

(c) Value of Restoration

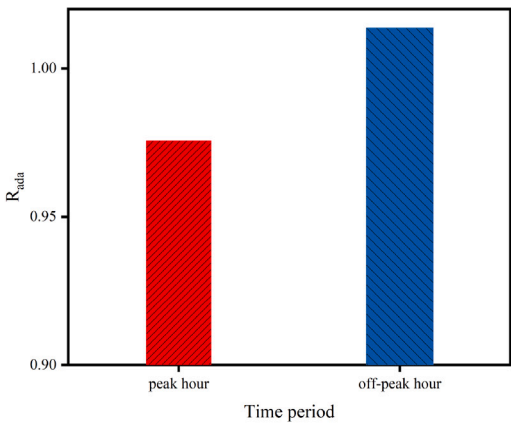

(d) Value of Adaptability

Fig. 8. Influence of saturation on MSR.

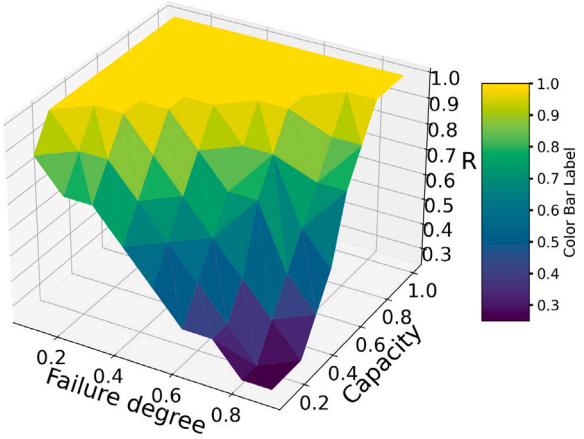

Fig. 9. Influence of failure degree and capacity on MSR.

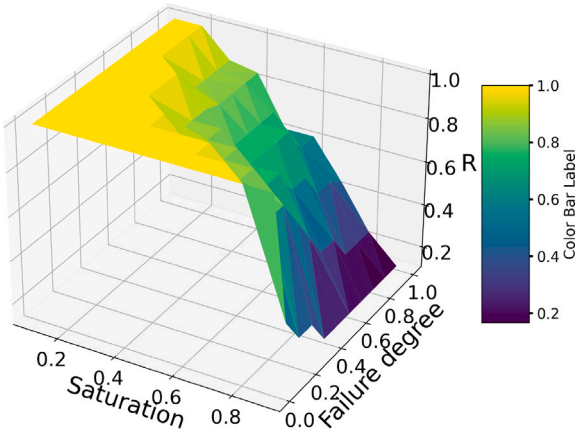

Fig. 10. Influence of failure degree and saturation on MSR.

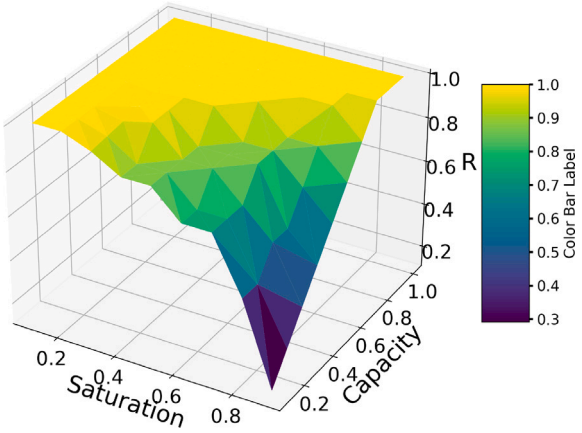

Fig. 11. Influence of capacity and saturation on MSR.

The findings reveal an inverse relationship between the degree of lane failures and MSR, while capacity is positively related to MSR. In addition, the cumulative resilience of single lanes is not equivalent to the resilience of road segments, which emphasizes the need for a dedicated analysis of lane failures.

This study provides insight into the dynamic evolution of MSR by examining the impact of failure degree, saturation, and capacity. The research shows that MSR remains unaffected by failures and oversaturation when capacity exceeds 0.8. However, within the capacity growth range of 0.1–0.7, the increase in failure degree and oversaturation leads to a decrease in the MSR. Furthermore, it is important to note that for the degree of failure exceeding 0.5 and saturations surpassing 0.7, the increase in MSR from adding capacity is minimal. Therefore, additional measures must be taken to improve the MSR.

In future research, the main analysis will consider pedestrians and non-motorized vehicles. Extending the MSR model to include pedestrians and non-motorized vehicles is necessary. Furthermore, optimizing traffic signal control is a complex field. In this study, an increase in the μ value means an increase in the green duration or cycle time. Subsequent analysis will explore optimizing signal timing in response to disturbances to improve system resilience. This exploration aims to optimize system resilience by optimizing signal timing in the affected area in response to disturbances. Future research can focus on optimizing the lane types to maximize overall network resilience while considering specific urban contexts and traffic patterns.

CRediT authorship contribution statement

Guizhen Chen: Writing – review & editing, Writing – original draft, Visualization, Methodology, Conceptualization. **Tom Van Woensel:** Writing – review & editing, Writing – original draft, Conceptualization. **Jinhua Xu:** Writing – review & editing, Data curation. **Yikai Luo:** Visualization, Data curation. **Yan Li:** Writing – review & editing, Writing – original draft, Conceptualization.

CRediT authorship contribution statement

Guizhen Chen: Conceptualization, Methodology, Visualization, Writing - original draft, Writing - review & editing. **Tom Van Woensel:** Conceptualization, Writing - original draft, Writing - review & editing. **Jinhua Xu:** Computation of manuscripts, Writing - review & editing. **Yikai Luo:** Visualization, computation of manuscripts. **Yan Li:** Conceptualization, Writing - original draft, Writing - review & editing.

Declaration of competing interest

No conflict of interest exists in the submission of this manuscript, and all authors approve the manuscript for publication.

Acknowledgments

This work is supported by the National Natural Science Foundation of China (No. 51408049), the Natural Science Basic Research Program of Shaanxi (2020JM-237), and the China Scholarship Council (No. 202206560017).

Data availability

Data will be made available on request.

References

[1] D. Abudayyeh, A. Nicholson, D. Ngoduy, Traffic signal optimisation in disrupted networks, to improve resilience and sustainability, Travel Behav. Soc. 22 (2021) 117–128.
[2] Z. Li, C. Jin, P. Hu, C. Wang, Resilience-based transportation network recovery strategy during emergency recovery phase under uncertainty, Reliab. Eng. Syst. Saf. 188 (2019) 503–514.
[3] J. Li, Y. Wang, J. Zhong, Y. Sun, Z. Guo, Z. Chen, C. Fu, Network resilience assessment and reinforcement strategy against cascading failure, Chaos Solitons Fractals 160 (2022) 112271.
[4] R.-R. Yin, H. Yuan, J. Wang, N. Zhao, L. Liu, Modeling and analyzing cascading dynamics of the urban road traffic network, Phys. A 566 (2021) 125600.
[5] M. SteadieSeifi, N.P. Dellaert, W. Nuijten, T. Van Woensel, R. Raoufi, Multimodal freight transportation planning: A literature review, European J. Oper. Res. 233 (1) (2014) 1–15.
[6] C. Ma, W. Hao, A. Wang, H. Zhao, Developing a coordinated signal control system for urban ring road under the vehicle-infrastructure connected environment, IEEE Access 6 (2018) 52471–52478.
[7] T.J. Dickson, A note on traffic assignment and signal timings in a signal-controlled road network, Transp. Res. B 15 (4) (1981) 267–271.
[8] Y. Li, J. Xu, Y. Li, Y. Xue, Z. Yao, Estimation and prediction of freeway traffic congestion propagation using tagged vehicle positioning data, Transp. B: Transp. Dyn. 12 (1) (2024) 2297143.
[9] N. Wang, M. Wu, K.F. Yuen, A novel method to assess urban multimodal transportation system resilience considering passenger demand and infrastructure supply, Reliab. Eng. Syst. Saf. 238 (2023) 109478.
[10] D. Henry, J.E. Ramirez-Marquez, Generic metrics and quantitative approaches for system resilience as a function of time, Reliab. Eng. Syst. Saf. 99 (2012) 114–122.
[11] M. Zhu, X. Huang, H. Pham, A random-field-environment-based multidimensional time-dependent resilience modeling of complex systems, IEEE Trans. Comput. Soc. Syst. 8 (6) (2021) 1427–1437.
[12] L. Zhang, J. Lu, B.-b. Fu, S.-b. Li, A cascading failures model of weighted bus transit route network under route failure perspective considering link prediction effect, Phys. A 523 (2019) 1315–1330.
[13] X. Zhang, S. Mahadevan, K. Goebel, Network reconfiguration for increasing transportation system resilience under extreme events, Risk Anal. 39 (9) (2019) 2054–2075.
[14] L.A. Elefteriadou, The highway capacity manual 6th edition: A guide for multimodal mobility analysis, ITE J.-Inst. Transp. Eng. 86 (4) (2016).
[15] F. Lu, K. Liu, Y. Duan, S. Cheng, F. Du, Modeling the heterogeneous traffic correlations in urban road systems using traffic-enhanced community detection approach, Phys. A 501 (2018) 227–237.
[16] C.D. Barros, M.R. Mendonça, A.B. Vieira, A. Ziviani, A survey on embedding dynamic graphs, ACM Comput. Surv. 55 (1) (2021) 1–37.
[17] J. Xu, Y. Li, W. Lu, S. Wu, Y. Li, A heterogeneous traffic spatio-temporal graph convolution model for traffic prediction, Phys. A 641 (2024) 129746.
[18] Y. Chen, Y. Guo, Y. Wang, Modeling and density estimation of an urban freeway network based on dynamic graph hybrid automata, Sensors 17 (4) (2017) 716.
[19] Z. Liu, H. Chen, E. Liu, W. Hu, Exploring the resilience assessment framework of urban road network for sustainable cities, Phys. A 586 (2022) 126465.
[20] J. Zhang, Z. Wang, S. Wang, W. Shao, X. Zhao, W. Liu, Vulnerability assessments of weighted urban rail transit networks with integrated coupled map lattices, Reliab. Eng. Syst. Saf. 214 (2021) 107707.
[21] S. Hong, J. Zhu, L.A. Braunstein, T. Zhao, Q. You, Cascading failure and recovery of spatially interdependent networks, J. Stat. Mech. Theory Exp. 2017 (10) (2017) 103208.
[22] M. Turalska, K. Burghardt, M. Rohden, A. Swami, R.M. D'Souza, Cascading failures in scale-free interdependent networks, Phys. Rev. E 99 (3) (2019) 032308.
[23] J. Pei, Y. Liu, W. Wang, J. Gong, Cascading failures in multiplex network under flow redistribution, Phys. A 583 (2021) 126340.
[24] Y. Zhang, Y. Lu, G. Lu, P. Chen, C. Ding, Analysis of road traffic network cascade failures with coupled map lattice method, Math. Probl. Eng. 2015 (1) (2015) 101059.
[25] C.S. Holling, Resilience and stability of ecological systems, Annu. Rev. Ecol. Syst. 4 (1) (1973) 1–23.
[26] P.M. Murray-Tuite, A comparison of transportation network resilience under simulated system optimum and user equilibrium conditions, in: Proceedings of the 2006 Winter Simulation Conference, IEEE, 2006, pp. 1398–1405.
[27] X. Fang, L. Lu, Y. Li, Y. Hong, A Driver-Pressure-State-Impact-Response study for urban transport resilience under extreme rainfall-flood conditions, Transp. Res. D 121 (2023) 103819.

[28] N.U.I. Hossain, F. Nur, S. Hosseini, R. Jaradat, M. Marufuzzaman, S.M. Puryear, A Bayesian network based approach for modeling and assessing resilience: A case study of a full service deep water port, Reliab. Eng. Syst. Saf. 189 (2019) 378–396.
[29] D. Bao, X. Zhang, Measurement methods and influencing mechanisms for the resilience of large airports under emergency events, Transp. A: Transp. Sci. 14 (10) (2018) 855–880.
[30] S.C. Calvert, M. Snelder, A methodology for road traffic resilience analysis and review of related concepts, Transp. A: Transp. Sci. 14 (1–2) (2018) 130–154.
[31] M. Bruneau, S.E. Chang, R.T. Eguchi, G.C. Lee, T.D. O'Rourke, A.M. Reinhorn, M. Shinozuka, K. Tierney, W.A. Wallace, D. Von Winterfeldt, A framework to quantitatively assess and enhance the seismic resilience of communities, Earthq. Spectra 19 (4) (2003) 733–752.
[32] S. Zhang, Y. Cheng, K. Chen, C. Ma, J. Wei, X. Hu, A general metro timetable rescheduling approach for the minimisation of the capacity loss after random line disruption, Transp. A: Transp. Sci. 20 (3) (2024) 2204965.
[33] Z. Shi, Z. Yang, J. Liu, et al., Assessing the dynamic resilience of local roads: A case study of flooding in Wuhan, China, J. Adv. Transp. 2022 (2022).
[34] E.D. Vugrin, D.E. Warren, M.A. Ehlen, A resilience assessment framework for infrastructure and economic systems: Quantitative and qualitative resilience analysis of petrochemical supply chains to a hurricane, Process Saf. Prog. 30 (3) (2011) 280–290.
[35] B. Bhavathrathan, G.R. Patil, Quantifying resilience using a unique critical cost on road networks subject to recurring capacity disruptions, Transp. A: Transp. Sci. 11 (9) (2015) 836–855.
[36] M.V. Martello, A.J. Whittle, J.M. Keenan, F.P. Salvucci, Evaluation of climate change resilience for Boston's rail rapid transit network, Transp. Res. D 97 (2021) 102908.
[37] X. Zhang, E. Miller-Hooks, K. Denny, Assessing the role of network topology in transportation network resilience, J. Transp. Geogr. 46 (2015) 35–45.
[38] Y. Liu, X. Ma, W. Qiao, L. Ma, B. Han, A novel methodology to model disruption propagation for resilient maritime transportation systems-a case study of the Arctic maritime transportation system, Reliab. Eng. Syst. Saf. 241 (2024) 109620.
[39] A.A. Ganin, M. Kitsak, D. Marchese, J.M. Keisler, T. Seager, I. Linkov, Resilience and efficiency in transportation networks, Sci. Adv. 3 (12) (2017) e1701079.
[40] Y. Wu, S. Chen, Resilience modeling and pre-hazard mitigation planning of transportation network to support post-earthquake emergency medical response, Reliab. Eng. Syst. Saf. 230 (2023) 108918.
[41] M. Akbarzadeh, S. Memarmontazerin, S. Derrible, S.F. Salehi Reihani, The role of travel demand and network centrality on the connectivity and resilience of an urban street system, Transportation 46 (2019) 1127–1141.
[42] P. Singh, A. Amekudzi-Kennedy, H. Kassa, Performance dashboard tool to visualize adaptive resilience maturity of transportation agencies, Transp. Res. Rec. 2676 (11) (2022) 324–339.
[43] S. Dong, X. Gao, A. Mostafavi, J. Gao, U. Gangwal, Characterizing resilience of flood-disrupted dynamic transportation network through the lens of link reliability and stability, Reliab. Eng. Syst. Saf. 232 (2023) 109071.
[44] W. Sun, P. Bocchini, B.D. Davison, Resilience metrics and measurement methods for transportation infrastructure: The state of the art, Sustain. Resilient Infrastruct. 5 (3) (2020) 168–199.
[45] S. Lhomme, D. Serre, Y. Diab, R. Laganier, Analyzing resilience of urban networks: a preliminary step towards more flood resilient cities, Nat. Hazards Earth Syst. Sci. 13 (2) (2013) 221–230.
[46] J.E. Muriel-Villegas, K.C. Alvarez-Uribe, C.E. Patiño-Rodríguez, J.G. Villegas, Analysis of transportation networks subject to natural hazards–Insights from a Colombian case, Reliab. Eng. Syst. Saf. 152 (2016) 151–165.
[47] S. Mudigonda, K. Ozbay, B. Bartin, Evaluating the resilience and recovery of public transit system using big data: Case study from New Jersey, J. Transp. Saf. Secur. 11 (5) (2019) 491–519.
[48] C. Chen, F. He, R. Yu, S. Wang, Q. Dai, Resilience assessment model for urban public transportation systems based on structure and function, J. Saf. Sci. Resil. 4 (4) (2023) 380–388.
[49] K. Gopalakrishnan, E. Koyuncu, H. Balakrishnan, et al., An empirical study of the resilience of the US and European air transportation networks, J. Air Transp. Manag. 106 (C) (2023).
[50] N. Mou, S. Sun, T. Yang, Z. Wang, Y. Zheng, J. Chen, L. Zhang, Assessment of the resilience of a complex network for crude oil transportation on the Maritime Silk Road, IEEE Access 8 (2020) 181311–181325.
[51] N. Wang, M. Wu, K.F. Yuen, Assessment of port resilience using Bayesian network: A study of strategies to enhance readiness and response capacities, Reliab. Eng. Syst. Saf. 237 (2023) 109394.
[52] Z. Ma, X. Yang, J. Wu, A. Chen, Y. Wei, Z. Gao, Measuring the resilience of an urban rail transit network: A multi-dimensional evaluation model, Transp. Policy 129 (2022) 38–50.
[53] D. King, A. Aboudina, A. Shalaby, Evaluating transit network resilience through graph theory and demand-elastic measures: Case study of the Toronto transit system, J. Transp. Saf. Secur. 12 (7) (2020) 924–944.
[54] Z. Xu, S.S. Chopra, H. Lee, Resilient urban public transportation infrastructure: A comparison of five flow-weighted metro networks in terms of the resilience cycle framework, IEEE Trans. Intell. Transp. Syst. 23 (8) (2021) 12688–12699.
[55] J. Wu, P. Liu, Y. Zhou, H. Yu, Stationary condition based performance analysis of the contraflow left-turn lane design considering the influence of the upstream intersection, Transp. Res. C 122 (2021) 102919.
[56] T. Urbanik, A. Tanaka, B. Lozner, E. Lindstrom, K. Lee, S. Quayle, S. Beaird, S. Tsoi, P. Ryus, D. Gettman, et al., Signal Timing Manual, vol. 1, Transportation Research Board, Washington, DC, 2015.